Tellus (1984), *36B*, 192–202

Size spectra of bubbles in the foam patches and of sea salt nuclei over the surf zone

By JOSEF PODZIMEK, *Graduate Center for Cloud Physics Research, University of Missouri-Rolla, 109 Norwood Hall, Rolla, MO 65401 USA*

(Manuscript received September 21, 1983; in final form February 7, 1984)

ABSTRACT

The size distribution of bubbles in the foam patches and the size distribution of giant chloride nuclei over the surf zone both follow the Nukiyama–Tanassava size distribution function. The slope of the size distribution curve for bubbles depends, however, on the residence time of the foam patch at the ocean surface. The best fit of the sea salt nuclei size distribution curve was found for $s = 0.333$ in the Nukiyama–Tanassava distribution.

1. Introduction

The surf zone is a prolific source of sea salt nuclei and salt solution droplets. They form a hazy layer over the seashore which extends on the sea breeze several hundred meters in altitude and many kilometers from the seashore over the continent (King and Maher, 1976; Radke, 1977; Blanchard and Woodcock, 1980; Podzimek, 1980a). The mechanism of the particle (droplet) generation at the seashore differs considerably from that identified, e.g., by Toba (1965), Chaen (1974), Blanchard and Woodcock (1980), or Koga (1981) on the free ocean surface. Besides bubble bursting, jet emission and droplet spraying where waves break and produce foam patches, one has to consider the interaction with the close bottom of the sea and the nuclei or drops generated at that part of the shore which is covered only temporarily by sea water.

The aforementioned mechanisms of salt nuclei generation at the seashore prompted an investigation into the size distribution of salt particles produced over a sand beach and its relationship to the size distribution of bubbles in foamy patches. No sophisticated theoretical explanation of the measured data is attempted. Instead, a simple size distribution function is sought for nuclei and bubbles. From the investigation of its form and time variability, it was hoped to obtain the information required to determine whether the bubble bursting and jet emission in the foam patches at the sand beach is the dominant mechanism of the salt particle generation.

2. Sampling site and instrumentation

Since 1975, two Texas seashore aerosol measurement programs were undertaken: in May 1975 on Padre Island ($\psi \simeq 27°$ N and $\lambda \simeq 97°$ W) over a sand beach of a typical barrier island and in January 1979 at the seashore of South Padre Island close to Port Isabel ($\psi \simeq 25°$ N and $\lambda \simeq 97°30'$ W). At both locations, Aitken nuclei (AN) concentrations were measured with the Gardner and General Electric counters, while particles with radii between approximately 0.1 μm and 5 μm were measured with a Royco counter (Model 225) and a PMS Knollenberg counter (Model ASAS-300A). Unico and Casella impactors were used for sampling and identification of the giant condensation nuclei of chlorides and sulfates. The same parameters were measured onboard an instrumented aircraft sampling at different altitudes several tens of miles over the continent and over the sea. The results of these measurements were described elsewhere (Podzimek 1977, 1980a, b)

with the exception of the results obtained from the study of the nature of the chloride nuclei generated over the decaying foam patches at the seashore.

Foamy patches formed by the wave action were photographed at approximately 5 s intervals 30–50 cm above the sandy bottom of the beach. The mean size of the patches varied between 0.1 and 0.5 m^2 and their mean lifetime was about 25 s for a sea breeze of 4–6 m s^{-1} and water of temperature 25.8 °C. The photographs were projected on a screen and evaluated with a mean error smaller than ±5% for bubbles with radii larger than 0.1 cm. The error increased considerably for bubbles smaller than 0.1 cm due to the uncertainty of defining the edge of the bubble, so that the minimum radius of the detected bubbles was around 0.03 cm. This minimum size does not completely cover the bubble size distribution below 0.05 cm to which Blanchard and Woodcock (1957), Day and Lease (1968), Kolovayev (1976) and Johnson and Cooke (1979) attributed the greatest rôle in bubble and salt nuclei generating mechanism. However, the size distribution of bubbles formed over a flat sand seashore always showed larger mean bubble diameters than those mentioned by the quoted authors. This also stresses the recent findings by Cipriano and Blanchard (1981) on the rôle of large bubbles in marine aerosol production.

Samples of the foam patch on a stainless steel plate were taken simultaneously. The salt particles which remained on the plate, after all the water was slowly evaporated in a controlled environment in the instrumented camper, were later examined in a scanning electron microscope. Their morphology and size distribution were recorded and the resulting distribution curves were compared with those for bubbles and airborne aerosol particles.

Aerosol particles were investigated in several ways. The main sampling was performed on the beach 60 m from the surf zone. Several samplings with cascade impactors were performed just above the surf zone (Podzimek 1973, 1980b). Usually, 1 or 2 min air samples were taken with a Unico impactor (at 16 l/min flow rate) placed approximately 1.5 m above the ground (sea bed) and approximately 15 cm above the sea water. Aerosol was deposited in the impactor on glass slides with a gelatin sheet sensitized for the detection of chloride- and sulphate-containing particles. Articles describing the preparation and evaluation of the spots (Liesegang circles) and the determination of the "magnification factors" have been published elsewhere (Podzimek, 1959; Preining et al., 1976; Yue and Podzimek, 1980). The evaluation of the circles in the sensitized gelatin sheets led to a determination of the complex structure of the salt embryos (Podzimek 1973, 1980b). For "pure" NaCl, the "magnification factor" can reach the value of 4.3 for a relative humidity (R.H.) of 82% and low salt concentration (1%), whereas for 72% R.H. and a droplet of initially 6% NaCl solution, it was around 2.08. For this reason, the humidity of the air was an important parameter measured during the aerosol sampling. The uncertainty of defining "dry" or "wet" salt nuclei according to the color of the circles is apparently the main deficiency of the spot-test technique, if one accepts the very laborious and time consuming evaluation of the samples. Finally, several aerosol samples were always taken with an electrostatic precipitator (TSI), used simultaneously with the cascade impactors, for later particle analysis in the electron transmission microscope.

3. Methodology and results of measurements

Many articles have been published on the mechanism by which sea salt nuclei are generated from a bursting bubble or jet emission (see the survey by Blanchard and Woodcock, 1980 or by Podzimek, 1980c). There is also some evidence that the size distribution curve for salt nuclei is directly related to the mechanism of nuclei generation (e.g., Moore and Mason, 1954; Woodcock, 1972) and that it might be deduced from the droplet and bubble-size distribution (Podzimek, 1977). The latter conclusion was reached after the laboratory experiments with salt solution and sea water (through which a controlled amount of clean air or nitrogen was bubbled) were performed. For the sake of easy modeling and in the light of the good fit to the measurements made previously at the seashore, the Nukiyama-Tanassava distribution of the type

$$\frac{dn}{dr} = Ar^2 \exp(-Br^4) \qquad (1)$$

was selected (Podzimek, 1973; Podzimek and Saad, 1974).

In this representation (Fig. 1), the curves for bubble (2), droplet (3) and salt nuclei (1) size distribution, plotted as $|\Delta N(r)/r^2\Delta r| = f(2r)$, show a similarity for the following size ranges: bubble diameters between 0.7 and 2.0 mm, droplet diameters between 7 μm and 20μm, and nuclei diameters from 0.7 μm to 2.0 μm. For sizes smaller than these lower limits, there is a considerable difference in the behavior of the droplet curve compared to the others, as it shows a clear decrease in concentration while the concentration of bubbles and generated nuclei is still increasing. However, both curves for small bubbles (in the domain $1.0 < d_b < 2.0$ mm) and nuclei (in the domain $1.0 < d_n < 2.0$ μm) have a different slope in comparison with the slope of the droplets for the size distribution curve (marked in Fig. 1). This was found during many laboratory experiments. During these experiments, the bubbles were generated 10 cm under the 3% salt solution level by bubbling pure nitrogen at a rate of 1–3 l/min through a fine frit. The bubbles were photographed in the generating flask 10 cm in diameter and evaluated after magnification in the TGZ 3 Zeiss Particle Size Analyzer. The drop concentration and size distribution was determined from the imprints in the gelatin layer (with a trace of napthol green the magnification factor was around 4.5) smeared on two microscope slides inserted into a four-stage Unico Impactor. The cascade impactor samples were taken 3 cm above the solution level through a 20 cm long and 1 cm I.D. tube at a flow rate of 16 l/min. Aerosol concentration and size distribution was measured with a PMS aerosol spectrometer, Model ASAS 300 A.

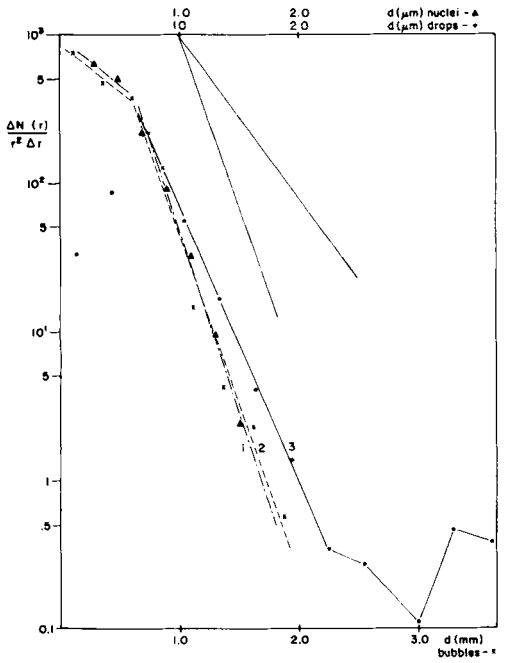

Fig. 1. Size distribution of aerosol particles (curve—1), bubbles (2) and droplets (3) produced by bubbling pure nitrogen gas through a 3% NaCl water solution. The curves are plotted as $\Delta N(r)/(r^2\Delta r) = f(2r)$. The light lines in the upper part of the figure represent the maximal deviations of the measured droplet size spectra slopes.

However, several problems of evaluating the bubble size spectrum from the photographs taken at the ocean surface have to be discussed before a meaningful explanation of the relationships to the size distribution of salt nuclei can be attempted. First, one has to ask whether the photographs of the surface of a foam patch truly reflect the bubble size distribution in the liquid's topmost layer which, by its nature, is a distribution of bubble volumes. Second, the most important parameters affecting the gas (vapor) transfer among bubbles have to be identified, in order to be able to compare the samples taken at different stages of foam patch evolution. Following Lemlich (1972), the main relationships of bubble population description and kinetics are mentioned in the Appendix.

From the photographs of the foam patches (Fig. 2), the mean values of surface bubble concentration, n_s, the bubble mean radius, $\bar{r}_s$, $\overline{r_s^2}$ and the mean bubble wall thickness, θ, were evaluated and the ratio of the liquid to gas volume, V_ℓ/V_g, and the factor of proportionality, K_s, calculated from eqs. (A4) and (A3). The data in Table 1 represent typical samples taken in the early afternoon hours on a sunny day. Because of the rapid variation with time of the bubble parameters, the samples were divided into three categories: Initial ($t < 5$ s), mature (5 to 10 s), and decaying (10 to 30 s) foam patch. In spite of the fact that each sample contained usually several hundred individual bubbles, there is a considerable error, approximately ± 15%, in determining the mean bubble wall thickness from the photographs.

Several simplifying assumptions have to be made in order to explain, at least qualitatively, the rapid alteration of the bubble size spectrum after the

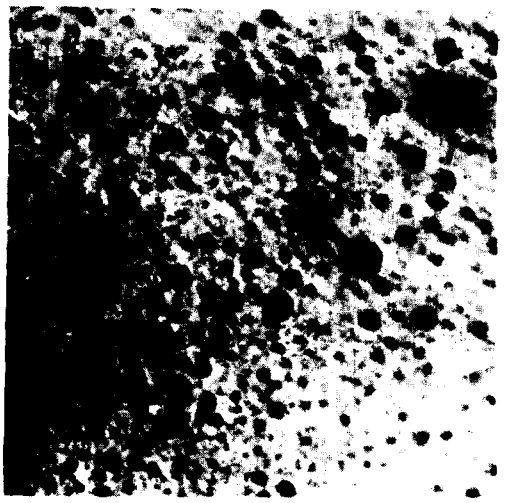

Fig. 2. Photograph of a mature foam patch. The photographed area corresponds to the true size of 5.0 cm × 5.0 cm.

foam patch appeared. In the appendix is mentioned: the random distribution of bubbles; the shrinkage of a very small bubble (with initial radius r_0) next to a very large one ($R \to \infty$), or adjacent to a gaseous environment; the constancy of parameters such as the factor of proportionality, K_s, for converting the surface bubble size distribution into a volume distribution; the gas permeability through the bubble liquid layer of a mean constant thickness, θ, etc. Assuming further that there is a constant bubble size distribution function $F(r_0)$, it is possible to calculate the rate of bursting bubbles from the total number of small bubbles, N_t, remaining from the original concentration, N_0, in the foam after a time, t:

$$N_t = N_0\left[1 - \int_0^{r_{0,t}} F(r_0)\mathrm{d}r_0\right]. \tag{2}$$

$r_{0,t}$ denotes the initial radius of bubbles, which after a time, t, burst or disappear. The bubble size distribution function is assumed to follow eq. (1), where the size parameter, B, in the exponent, has the dimension of r^{-s}. Because eq. (1) represents a gamma distribution, one can write it in the form

$$\frac{\mathrm{d}n}{\mathrm{d}r} = \frac{sB^{3/s}}{\Gamma(3/s)} r^2 \exp(-Br^s), \tag{3}$$

which shows the special meaning of the parameter, A, in eq. (1). The corresponding bubble (spherical) volume distribution is then (Mugele and Evans, 1951)

$$\frac{\mathrm{d}v}{\mathrm{d}r} = \frac{B^{6/s}}{\Gamma(6/s)} r^5 \exp(-Br^s). \tag{4}$$

From eqs. (2), (3) and (A6) one can find the relationship between N_t and t, and answer the question of how many bubbles will survive in the foam patch after a time, t. If the patch is sufficiently large, one can assume the homogeneous size distribution of "spherical" bubbles and justify the steady form of the size distribution function $F(r_o)$ in eq. (2). Then, rearranging the function $F(r_o)$ and integrating the individual terms for specific values of s (e.g. $s = 1.0$), the curves $(N_t/N_0) = f(t)$ were plotted in Fig. 3. For the calculation of the main parameters, such as B, τ [defined by eq. (1) and (6A)], Table 1 and the slopes of the lines in Figs. 4, 5, and 6 were used. τ was calculated for $T = 293$ K; $\sigma = 72.8 \times 10^{-2}$ Nm^{-1}; $P = 1.0526 \times 10^{-5}$ and 4.4494×10^{-8} m s^{-1}; $p_a = 1.013 \times 10^{-3}$ Nm^{-2}. This yields approximately $\tau \simeq 1.0897$ and $\tau \simeq 2.5779$ as the two extreme values obtained from our observations. In spite of considerable uncertainties concerning the bubble wall thickness and the values of D and S, the mean times of observed completely shrinking foamy patches are consistent with the calculated bubble lifetimes in Fig. 3.

Table 1. *Main parameters of foam patches at the beach corresponding to different stage of the fast evolving patch (samples from May 21, 1975, 13:30)*

Type of the patch	n_s (cm^{-2})	$\bar{r}_s$ (cm)	$\bar{r}_s^2$ (cm)	θ (cm)	V_c/V_s	K_s
Initial $t < 5$ s	23.22	0.0599	0.0036	0.0317	0.7912	0.3136
Mature $5 < t < 10$ s	21.17	0.0809	0.0065	0.0190	0.3044	0.4395
Decaying $10 < t < 30$ s	6.00	0.2027	0.0411	0.0445	0.3292	0.6865

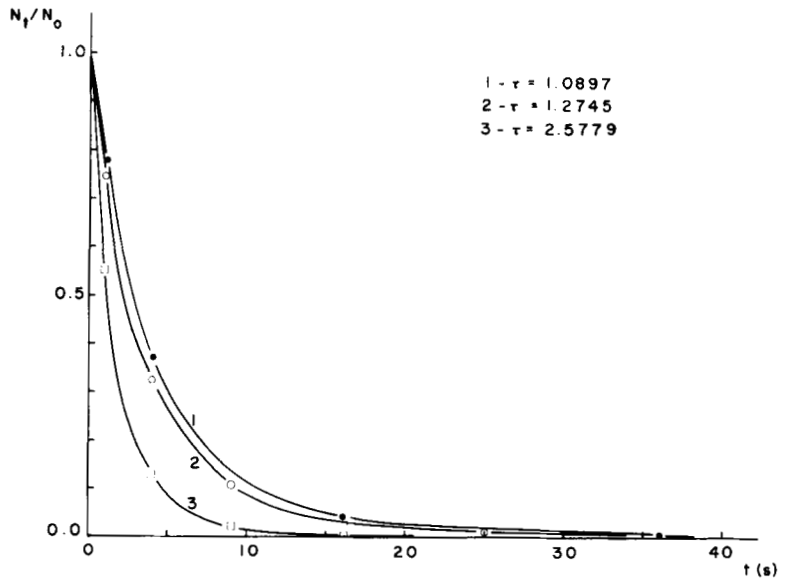

Fig. 3. Calculated "decay" curves of a model population of bubbles for a given bubble size distribution ($\Delta N(r) = Ar^2 \exp(-Br^s)\Delta r$; $s = 1.0$) and parameters τ deduced from the observation of foam patches at the seashore.

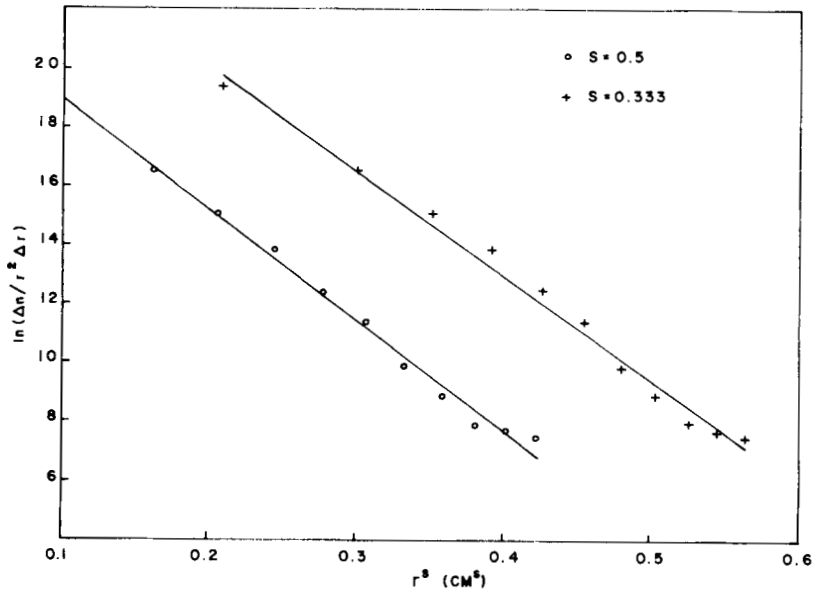

Fig. 4. Evaluated bubble size distribution (patch no. 1, 21 May 1975); R.H. = 84%.

Apparently, the largest deviations from this picture one can anticipate will occur at the beginning of the process when bubbles are rising with different velocity to the water surface. In this initial stage, the bubbles coalesce (rupture) intensely and larger bubbles entrain the smaller ones to the surface layer (Lemlich, 1972, p. 30; Thorpe, 1982; Zheng et al., 1983).

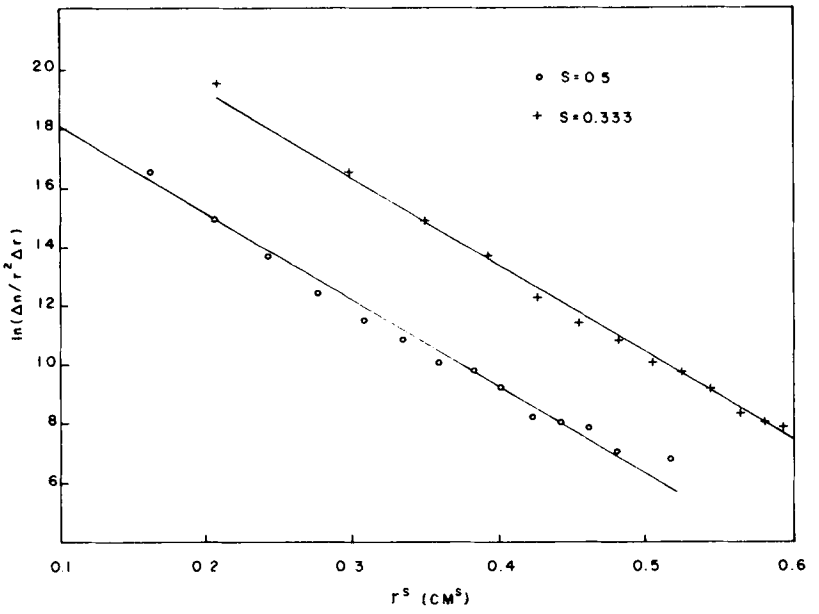

Fig. 5. Evaluated bubble size distribution (patch no. 6, 21 May 1975); R.H. = 83%.

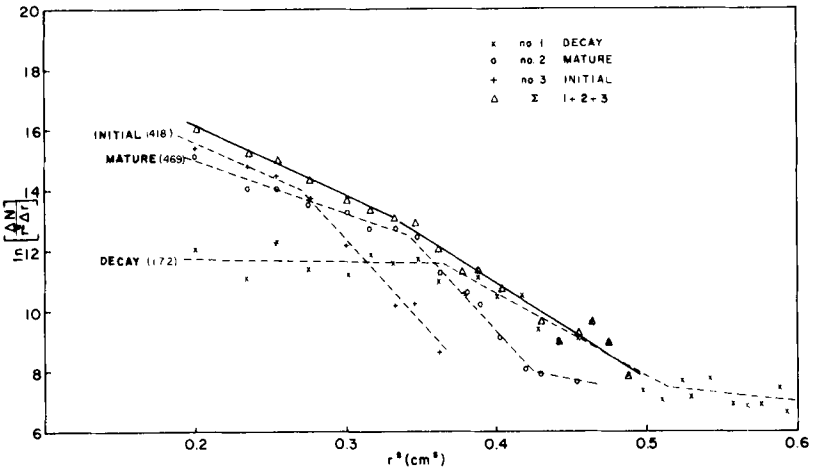

Fig. 6. Integrated bubble size distribution curve (full line) and the curves describing the initial, mature and decay stage of the same foam patch at the seashore (patch no. 2, 21 May 1975); R.H. = 84%.

4. Results of observations and measurements

The measured bubble diameters were divided into radius class intervals of $\Delta r = 0.015$ cm for the size range 0.04 cm $< r <$ 0.4 cm. Because of the form of eq. (1) and the need to evaluate the slope of the curve of the monotonically decreasing function, the original expression can be recast in the following, logarithmic, form

$$\ell n\left(\frac{1}{r^2}\frac{dn}{dr}\right) = \ell n\, A - Br^s. \tag{5}$$

By plotting $\ell n(r^{-2}dn/dr)$ versus r^s, it was possible to determine the slope of the line (the value of B)

and A. Simultaneously, the best fit with an ideal line was sought by changing the value of s (e.g., 1; 0.5; 0.33).

Two examples out of 10 series of time lapse photographs representing 10 shrinking foamy patches are evaluated in Figs. 4 and 5. Both show a reasonably good fit with the Nukiyama-Tanassava (N.T.) distribution with a slope of the lines in Figs. 4 and 5 corresponding approximately to 145°. Both values of s (i.e., 0.5 and 0.333) yield a good approximation. Because each figure corresponds to approximately 800 bubbles counted on several photographs taken during the whole lifetime of the foamy patch, a very interesting question arose as to whether the different stages of evolving and shrinking foam are not characterized by a specific bubble size distribution function. The photographs taken several seconds after the foam patch emerged at the surface (initial stage), after 10 s (mature stage) and after 20 s (decay) are evaluated separately in Fig. 6. The curves plotted show clearly that the bubble populations do not follow the N.T. size distribution function (the number of bubbles counted is given in parenthesis at each stage); however, integrated over the lifetime of the foam patch, the curve approaches the N.T. distribution (for $s = 0.50$).

The comparison between the bubble size distribution, integrated over a lifetime of a foamy patch, and the size distribution of salt nuclei deposited on a stainless steel plate after the seawater from the foam sample evaporated is presented in Fig. 7. The size distribution of deposited salt nuclei (which might simulate the effect of a foam patch evaporation on the beach) was evaluated in a scanning electron microscope. Both populations, bubbles and deposited salt particles, follow well the N.T. distribution function for $s = 0.5$ up to the radii of salt nuclei of 4.0 μm.

During the period of bubble photography, salt aerosol particles with $r > 1.0$ μm were sampled with the aid of cascade impactors which were placed 60 m from the surf zone (1.5 m above the sand beach) and 20 cm above the water in the surf zone (Podzimek et al., 1978). The nature and size of salt nuclei were determined by the Liesegang circle technique already described. The size distribution curves in Fig. 8 follow well the N.T. distribution function on both sites, especially, if $s = 0.333$ is used. There is, however, an indication that the curves for $s = 0.333$ change their slopes at

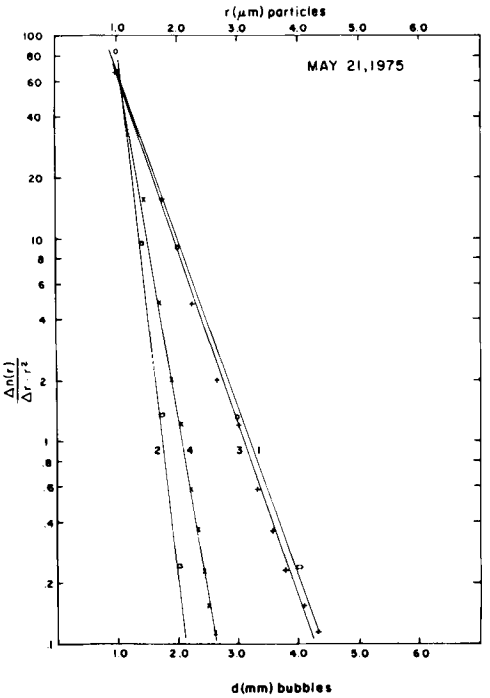

Fig. 7. Size distribution curves for bubbles photographed in the foamy patch and salt particles remaining on the stainless steel plate after the water evaporated. Curve 1: N.T. distribution for bubbles ($s = 1.0$); curve 2: the same for $s = 0.5$; curve 3: deposited salt particles ($s = 0.5$); curve 4: deposited salt particles for $s = 0.333$.

$r' = 1.5$ μm. The curve for the campsite (1 in Fig. 8) is shifted toward smaller nucleus sizes, if compared with the nuclei size distribution measured directly over the surf zone. This reveals that the droplet evaporation and salt nuclei crystallization process lasts for tens of seconds, if one can neglect the sedimentation of particles.

5. Discussion of the results

This investigation is concerned with the size distribution of bubbles and salt particles generated in the laboratory and in foam patches at the seashore.

Bubbling of nitrogen through a salt solution is considered by several authors (e.g., Cipriano and Blanchard, 1981; Monahan, 1982) as an imperfect simulation of the bubble and aerosol formation in the whitecaps. However, the laboratory measure-

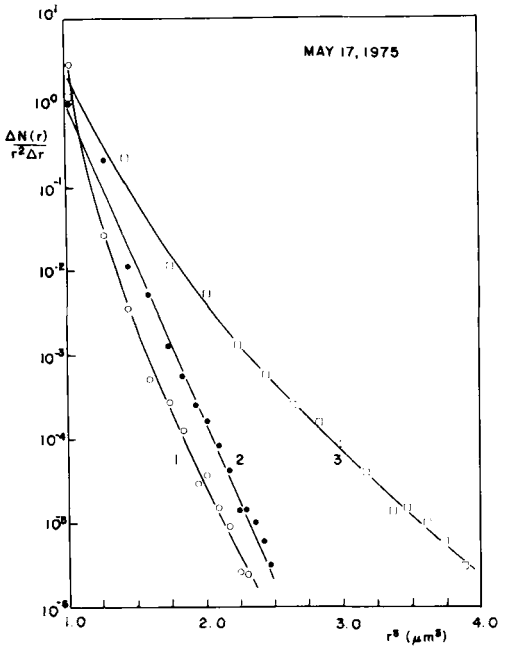

Fig. 8. Size distribution curves for a sea salt aerosol sampled 150 cm above the sand beach 60 m from the surf zone (curve 1: for $s = 0.333$) and aerosol sampled 150 cm above the surf water (curve 2: for $s = 0.333$; curve 3: for $s = 0.5$); R. H. = 67%.

ments described, consistent with observation in nature, led to the conclusion that both bubble and salt aerosol size distribution can reasonably well be described by a simple distribution function. This was found earlier by several authors who performed the measurements in the laboratory and in the field. Using a simple power law (Junge's formula $dN/dr = Cr^{-\beta}$), Monahan (1982) published a survey of values for β obtained by different authors. The range of β-values is wide, from 1.5 to 4.8. Interestingly enough is the fact that, after converting the laboratory bubbling experiments described in this study into Junge's distribution, one obtains $\beta = 4.30$. The same procedure applied for the evaluation of the photographs of May 21, 1975 from the Texas seashore (Fig. 6), yields the value $\beta = 4.17$. The Junge distribution could not be applied for bubble sizes smaller than 0.07 cm and, in general, it seems that it is not as close to the measured data as the N.T. distribution. The exponent β for salt aerosol particles produced by the bubbling as described earlier, yielded $\beta = 4.50$ for particle diameters larger than 0.7 μm. However, for nuclei with diameters less than 0.7 μm, one observes a slight change in the slope of the size distribution curve corresponding to $\beta < 4.0$.

The technique used in this study, as mentioned previously, is simple photography of the bubbles of the foamy patch. More sophisticated instrumentation was used by several authors who performed investigations of the bubble size distribution beneath the ocean surface. An acoustic technique (Medwin, 1970), a bubble trap (Blanchard and Woodcock, 1957; Kolovayev, 1976) and an underwater photographic camera (e.g., Johnson and Cooke, 1979) are mentioned in the literature. It was found that near the sea surface, bubble population decreases exponentially with depth and that the bubble size spectrum can be described by a special type of Junge relationship $n \sim r^{-\beta}$ (Wu, 1981). In well-developed whitecaps, Medwin (1970) found $\beta = 4$ for bubbles with $r < 80$ μm, and $\beta = 2$ for large bubbles ($r > 80$ μm); Kolovayev (1976) obtained $\beta = 3.5$ and Johnson and Cooke (1979) $\beta = 5.0$ for the portion of the large bubble spectrum.

The bubble size distribution function applied in this study is more complicated than the Junge-type formulas or the log-normal distribution used by several investigators for the bubble size distribution models in spraying devices (e.g., Rudis and Jezdinsky, 1976). However, it determines in a simple way the cumulative volume fraction of particles in the form of a ratio of incomplete and complete gamma functions:

$$V = \int_0^{Br'} x^{6/s-1} e^{-x} dx \Big/ \int_0^{\infty} x^{6/s-1} e^{-x} dx$$

$$\equiv \Gamma_{Br'}\left(\frac{6}{s}\right) \Big/ \Gamma\left(\frac{6}{s}\right). \qquad (6)$$

This special type of gamma distribution describes well spray and cloud-droplet size distribution, and was also found suitable for particulates produced by mechanical grinding. The variable parameters in eq. (1), such as A, B, s (one of these parameters, A, can be eliminated), offer a unique combination for describing a specific bubble- or aerosol-generating process. There is enough evidence to conclude that for the description of the bubble size distribution in foamy patches at the seashore, the values of $s = 0.5$ or $s = 0.333$ fit best with the

measurements (Podzimek et al., 1978). However, one should emphasize that for a representative sample, it is necessary to evaluate all stages of the evolution of the bubble size spectrum. The initial and decay stages deviate considerably from the ideal mean bubble size distribution.

Laboratory and field measurements support the idea that for a specific size range, both the bubbles and the droplets emitted by bursting bubbles follow the N.T. distribution function. The best fit for bubbles was found for $s = 0.4$, and for aerosol (in the size range $0.7\ \mu m < 2r < 2.0\ \mu m$) for $s \simeq 0.33$–0.50 (Fig. 1). The droplets emitted by bursting bubbles approximately followed the distribution line with $s = 0.50$ except for diameters smaller than $0.8\ \mu m$ and larger than $2.2\ \mu m$. This sudden change of size distribution of in-laboratory produced small droplets, paralleled by a change of the slopes of the curves for nuclei and bubbles, might be related to a change in the basic mechanism of droplet generation or sampling (Fig. 1). In nature, this dramatic change in size distribution was not found if the whole life process of the foamy patch was considered (Figs. 4 to 6). The laboratory findings (Fig. 1) do not contradict the experiments by Cipriano and Blanchard (1981) who suggested that most of the droplets smaller than 5–10 μm in diameter originate as film drops after the bubble rupture. The number of film drops generated by a 2 mm bursting bubble is around 100 and this number strongly increases with bubble size. This is supported by a not-so-steep slope of the droplet size distribution curve (no. 3 in Fig. 1) and by a sudden increase of the concentration of droplets (with diameter around 3.5 μm) produced by a few bubbles with diameters larger than 2.0 mm.

The size distribution of giant salt nuclei (and also of salt particles deposited on a substrate) is well described with an N.T. function with the parameter $s = 0.5$ or $s = 0.33$. On many occasions, however, a strong increase was found in nucleus concentration for particles with $r \leqslant 1.0\ \mu m$ in nature in contradiction with the laboratory experiments (Fig. 1). Because this broken size distribution curve was found not only on the beach (e.g., Podzimek, 1973, 1980c) but also in higher levels over the seashore (Podzimek and Stampfer, 1977), one can conclude that it is a specific characteristic of an aerosol produced at the beach. Several problems related to the evaluation of Liesegang circles formed in a sensitized gelatin layer by small salt nuclei have been discussed elsewhere (Yue and Podzimek, 1980).

6. Conclusion

The prolific production of sea salt aerosol along a flat seashore is apparently caused by the combined effect of bubble bursting (film and jet droplets), by the droplet production over the breaking waves and by droplet evaporation on the sand beach. The shrinking of bubbles in a foamy patch is a fast process which lasts several tens of seconds. The foam patch bubble curve was reasonably well described by the Nukiyama-Tanassava (N.T.) distribution function with a parameter s around 0.4 (eq. 1). However, the sampling ought to include all three main stages of a foamy patch evolution in order to obtain the best fit with the N.T. function, but this was only applied to bubbles with diameters larger than 5.0×10^{-2} cm. In comparison with other data published, e.g., in Lemlich (1972), one finds the bubble wall thickness larger in the mean than in other studies, which might be due to the simple photographic technique used in this study. The technique, however, seems to be quite acceptable for bubbles larger than 5.0×10^{-2} cm which play a dominant rôle in seasalt cloud-condensation nuclei generation.

The giant sea salt nuclei and particulates deposited on a substrate also follow well the N.T. distribution function with the best-fit for $0.33 < s < 0.50$. All three parameters defining this distribution can easily be determined from the measurements. There is still some uncertainty in the magnification factor and evaluation of Liesegang circles of dry salt nuclei with radii $r \leqslant 1.0\ \mu m$. One does not yet know the explanation of the broken curves for small nuclei ($r \simeq 1.0\ \mu m$) which characterize the description of the aerosol samples from the beach.

7. Acknowledgement

The author is indebted to Professor O. Preining and to Mrs. M. Podzimek for their help in photographing the foamy patches and measuring the sea salt nuclei concentration during field trips to the Texas seashore in 1975 and 1979. Mrs. Vickie Maples ably assisted in preparing the manuscript

for printing. The financial support of the investigation by the National Science Foundation, Washington, D.C. (Grant ATM77-22173) is appreciated.

8. Appendix

One usually postulates that the bubbles are randomly distributed in the surface foam layer, the volume of which is defined by a unit area times the bubble diameter (Lemlich, 1972, p. 14). Further, it is assumed that a factor of proportionality, K_s, exists, by which one multiplies the bubble volume distribution in order to convert it into a surface (of unit area) distribution. Then

$$n_s f(r_s)\mathrm{d}r_s = 2rK_s NF(r)\mathrm{d}r, \tag{A1}$$

where n_s and N are the total bubble numbers per unit area and volume. Integrating eq. (A1) from r_s, $r = 0$ to r_s, $r = \infty$ (r_{max}) one obtains

$$n_s = 2K_s N\bar{r} \equiv \frac{3K_s}{2\pi}\,\frac{V_g}{V_g + V_\ell}\,\frac{\bar{r}}{\overline{r^3}}. \tag{A2}$$

$\bar{r}$, $\overline{r^3}$ are the mean (linear) radius and the mean volume radius of the bubble distribution. V_g, V_ℓ are gas and liquid volumes in the total volume of the foamy patch. From eq. (A2), the factor of proportionality, K_s, can be calculated if the relationships between the higher size distribution moments (e.g., $\bar{r}^{-1} = \overline{r_s^{-1}}$; $\overline{r^2} = \overline{r_s}/\overline{r_s^{-1}}$; $\overline{r^3} = \overline{r_s^2}/\overline{r_s^{-1}}$) are known;

$$K_s = \frac{2\pi n_s \overline{r_s^2}}{3}\left(1 + \frac{V_\ell}{V_g}\right). \tag{A3}$$

The ratio of liquid to gas volume reverts to a simple form

$$\frac{V_\ell}{V_g} = \frac{3\theta r_s}{2\overline{r_s^2}} \tag{A4}$$

in the case of a spherical bubble if θ is the average bubble wall thickness. A more general formula was published for polyhedral foam bubbles by Lemlich (1972, p. 16). Eqs. (A1)–(A4) enable us to convert a surface bubble size distribution into a volume distribution if the parameter K_s has been determined from the photographs. Accordingly, Table 1 presents the results of the evaluation made separately for each different stage of an evolving patch in shallow water at a sand beach.

The evolution of a foamy patch can be described under several simplifying assumptions, thus obtaining a rough idea as to which parameters play a dominant rôle in characterizing the samples at different times after the patch emerged on the agitated sea surface. Lemlich (1972, p. 15) assumed the shrinkage of a very small bubble of radius r in the presence of a very large bubble ($R \to \infty$). A mixture of water vapor and air is handled as an ideal gas and the gas pressure difference between the small and large bubble is approximated by a relationship $\Delta p_{1,2} = 2\sigma(1/r - 1/R) \simeq 2\sigma/r$. This leads to the well-known bubble growth (shrinkage) equation in the form

$$-r\frac{\mathrm{d}r}{\mathrm{d}t} = 2\sigma P\left(\frac{RT}{p_a}\right). \tag{A5}$$

Integrating eq. (A5), one can calculate the lifetime of a small bubble with an initial radius r_0:

$$t(r_0) = \frac{p_a}{4RT\sigma P} r_0^2 \equiv \tau r_0^2. \tag{A6}$$

In eqs. (A5) and (A6), σ is the surface tension of the liquid, p_a is the ambient atmospheric pressure (much larger than the excess pressure in the bubble), R is the gas constant, T the absolute temperature and P is the gas permeability through the bubble liquid layer of thickness θ. The latter is usually defined as

$$P = \frac{DS}{(\theta + 2D/k_i)}, \tag{A7}$$

where D is the diffusion coefficient of the gas in the liquid, S is the solubility of the gas in the liquid and k_i is the coefficient characterizing the mass transfer process across the gas liquid interface. Because from the evaluated photographs $\theta > 10^{-4}$ cm and for air $2D/k_i \sim 2 \times 10^{-6}$ cm, one can assume $P \sim DS/\theta$. The value of the permeability, P, for air transfer through the water bubble wall of mean thickness $\theta \simeq 1.9 \times 10^{-2}$ cm to 4.45×10^{-2} cm was close to 10^{-5} cm s^{-1}. This value was used for the calculation of the number of small bubbles (N_t) which will remain from their original concentration, N_0, in the foam patch after a time t.

REFERENCES

Blanchard, D. C. and Woodcock, A. H. 1957. Bubble formation and modification in the sea and its meteorological significance. *Tellus 9*, 145–158.

Blanchard, D. C. and Woodcock, A. H. 1980. The production, concentration, and vertical distribution of the sea salt aerosol. *Ann. New York Acad. Sci. 338*, 330–347.

Chaen, M. 1974. Studies of the production of sea salt particles on the sea surface. *Mem. Fac. of Fisheries, Kagoshima Univ. 22*, 49–107.

Cipriano, R. J. and Blanchard, D. C. 1981. Bubble and aerosol spectra produced by a laboratory "breaking wave". *J. Geophys. Res. 86*, 8085–8092.

Day, J. A. and Lease, J. C. 1968. Cloud nuclei generated by bursting air bubbles at the air–sea interface. *Proc. Int. Conf. on Cloud Physics, Toronto*, Univ. of Toronto, 20–24.

Johnson, B. D. and Cooke, R. C. 1979. Bubble populations and spectra in coastal waters: a photographic approach. *J. Geophys. Res. 84*, 3761–3766.

King, W. D. and Maher, C. T. 1976. The spatial distribution of salt particles at cloud levels in Central Queensland. *Tellus 28*, 11–23.

Koga, M. 1981. Droplet distribution and dispersion processes on breaking wind waves. *Sci. Rep. Tohoku Univ. Ser. 5, 28*, 1.

Kolovayev, D. A. 1976. Investigation of the concentration and statistical size distribution of wind-produced bubbles in the near-surface ocean. *Oceanol.* (English Translation) USSR *15*, 659–661.

Lemlich, R. 1972. *Adsorptive bubble separation techniques*. Academic Press, New York.

Medwin, H. 1970. In situ acoustic measurements of bubble populations in coastal ocean waters. *J. Geophys. Res. 75*, 599–611.

Monahan, E. C. 1982. Comment on 'Bubble and aerosol spectra produced by a laboratory breaking wave', by R. J. Cipriano and D. C. Blanchard. *J. Geophys. Res. 87*, 5865–5867.

Moore, D. J. and Mason, B. J. 1954. The concentration, size distribution, and production rate of large salt nuclei over the oceans. *Q. J. Roy. Meteorol. Soc. 80*, 583–590.

Mugele, R. A. and Evans, H. D. 1951. Droplet size distribution in sprays. *Ind. Engin. Chem. 43*, 1317–1324.

Podzimek, J. 1959. Measurement of the concentration of large and giant chloride condensation nuclei during flight. *Stud. Geophys. et Geod. 3*, 256–280.

Podzimek, J. 1973. Contribution to the question of condensation nuclei formation on the seashore. *J. Rech. Atmos. 7*, 137–152.

Podzimek, J. 1977. Comparison of sodium chloride particles generated in the laboratory and in nature. *J. Rech. Atmos. 11*, 227–238.

Podzimek, J. 1980a. The influence of aerosol inhomogeneity on cloud formation in coastal region. *J. Rech. Atmos. 14*, 241–253.

Podzimek, J. 1980b. Seashore aerosol at high relative humidity. Preprint Vol. *Second Conf. on Coastal Meteorology, Los Angeles*, Jan. 1980, AMS, Boston, 129–135.

Podzimek, J. 1980c. Advances in marine aerosol research. *J. Rech. Atmos. 14*, 35–61.

Podzimek, J., Preining, O., Russel, C. A. and Stampfer, J. F. 1978. *Aerosol studies at the Texas seashore.* Tech. Rep. no. AG-8, Graduate Center for Cloud Physics Research, Univ. of Missouri-Rolla, February (available from GCCPR, UMR, Rolla, MO 65401).

Podzimek, J. and Stampfer, J. F. 1977. *Vertical distribution of maritime aerosol above the seashore.* Tech. Rep. No. AG-7, Graduate Center for Cloud Physics Research, Univ. of Missouri-Rolla, July (available from GCCPR, UMR, Rolla, MO 65401).

Podzimek, J. and Saad, A. N. 1974. Evolution of giant chloride nuclei size spectrum on the seashore. *Arch. Met. Geophys. Bioklim., Ser. A, 23*, 77–86.

Preining, O., Podzimek, J. and Yue, P. 1976. The magnification factor for sodium chloride Liesegang circles established with an aerosol centrifuge. *J. Aerosol Sci., 7*, 351–358.

Radke, L. F. 1977. Marine aerosol: simultaneous size distributions of the total aerosol and the sea salt fraction from 0.1 to 10 μ diameter. *Proc. 9th Int. Conf. on Atmospheric Aerosols, Cond. and Ice Nuclei, Galway*, in *Atmospheric Aerosols and Nuclei* (eds.: A. F. Roddy and T. C. O'Connor), Galway Univ. Press, 1981, 487–491.

Rudis, M. and Jezdinsky, V. 1976. Distribution of bubble magnitude from a rotating sparger. *Z. Angew. Math. Mech. 56*, 486–489.

Thorpe, S. A. 1982. On the clouds of bubbles formed by breaking wind waves in deep water, and their rôle in air–sea gas transfer. *Phil. Trans. R. Soc. London, A304*, 155–210.

Toba, Y. 1965. On the giant sea salt particles in the atmosphere (II). Theory of the vertical distribution in the 10 m layer over the ocean. *Tellus 17*, 365–382.

Woodcock, A. H. 1972. Smaller salt particles in oceanic air and bubble behavior in the sea. *J. Geophys. Res. 77*, 5316–5321.

Wu, J. 1981. Bubble populations and spectra in near surface ocean: summary and review of field measurements. *J. Geophys. Res. 86*, 457–463.

Yue, P. C. and Podzimek, J. 1980. Potential use of chemical spot test method for submicron aerosol sizing. *Ind. Eng. Chem. Prod. Res. Dev. 19*, 42–46.

Zheng, Q. A., Klemas, V. and Hsu, Y.-H. L. 1983. Laboratory measurement of water surface bubble life time. *J. Geophys. Res. 88*, 701–706.